

Electrochemical Hydrodynamics Modeling Approach for a Copper Electrowinning Cell

K.R. Kim^{1,*}, S.Y. Choi¹, S. Paek¹, J.Y. Park², I.S. Hwang², and Y.Jung³

¹ Korea Atomic Energy Research Institute, 1045 Daedeok-daero, Yuseong-gu, Daejeon, 305-353 Korea

² Department of Nuclear Engineering, Seoul National University, Sillim-dong, Gwanak-gu, Seoul, 151-742, Korea

³ Department of Chemical Engineering, Korea University of Technology and Education, Cheonan, 330-780, Korea

*E-mail: krkim1@kaeri.re.kr

Received: 24 June 2013 / *Accepted:* 18 August 2013 / *Published:* 25 September 2013

This study demonstrates a simulation based on a full coupling of electrochemical kinetics with the 3-dimensional transport of ionic species in a flowing electrolyte through a simplified channel cell of copper electrowinning. The dependences of ionic electro-transport on the velocity of a stationary electrolyte flow were studied using a coupling approach of the electrochemical reaction model. The present model was implemented in a commercially available computational fluid dynamics (CFD) platform, Ansys-CFX, using its customization ability through user-defined functions. The main parameters characterizing the effect of the turbulent flow of an electrolyte between two planar electrodes were demonstrated by means of a CFD-based multiphysics simulation approach. Simulation was carried out for the case of the mass transport controlled copper electrowinning characteristics in a stream of acid sulfate electrolyte. This approach was taken into account in the concentration profile at the electrode surface, to represent the variation of the convective diffusion limited current density as a function of the flow characteristics and of the applied current density. It was able to predict a conventional current-voltage relation in addition to details of the electrolyte fluid dynamics and electrochemical variable, such as the flow field, species concentrations, potential, and current distributions throughout the galvanostatic cell.

Keywords: Computational fluid dynamics (CFD), Electrochemical hydrodynamics, Electrochemical system simulation, Electro-transport, Copper electrowinning.

1. INTRODUCTION

The importance of the computer simulations in the design and performance assessment of electrochemical systems has increased dramatically during the last three decades. The electrolysis

model provides engineers the ability to simulate the influence of the cell geometry and operating conditions in the electrochemical metallurgy industry [1, 2, 3, 4, 5].

The electrochemical reaction based on the hydrodynamics of the flowing electrolyte in an electrometallurgical cell is a complex, highly non-linear coupled phenomenon. The effect of the flow field to the electrode reaction in an electrolyte domain is the result of a combination of various hydrodynamics and mass transport [6, 7, 8]. The electrometallurgical efficiency and quality are determined by the cell configuration, operating conditions (mixing, applied current and cell voltage), and chemical state of the electrolytic cell. The ion current in the bulk electrolyte requires knowledge of the electrode surface, which requires an electrochemical hydrodynamics analysis of a mixing and mass transport.

The most effective way to accelerate the development of these technologies is to formulate physical models of the underlying electrochemical and transport processes. In addition, an integrated multiphysics simulation offers an efficient approach to designing, testing, and implementing these processes [9, 10].

A copper electroplating system has recently become the reference and standard technique for metalizing interconnects in high-end electrodeposition studies [11]. This established system enables a wide range of electrochemical features to be achieved in a single experiment and is useful to benchmark a proposed model. In addition, a reliable database of copper electrode reaction kinetics has been made available and provides an important parametric analysis for the simulation capability [12, 13].

In this study, an electrochemical hydrodynamics modeling approach based on a mass-transport controlled electrode reaction using a commercial computational fluid dynamics (CFD) platform was proposed. We demonstrated for the application of theoretical modeling to the copper electrowinning processes in an acid electrolyte flow channel involving both convective and diffusive transport. The applications discussed herein involve the use of computational multiphysics modeling to aid in the development of these systems, and to provide a theoretical framework for predicting electrochemical behavior in a future innovative process.

2. MODEL AND ELECTROWINNING CELL

2.1. Modeling approach

A commercial ANSYS[®]-CFX code [14] was employed to solve the electrochemical hydrodynamics model in a given electrochemical cell geometry. The finite-volume incompressible Navier–Stokes and transport equations were solved to obtain the ionic species concentrations and electric field at each position in the cell. A scalar transport equation was used to describe the electro-transport of the reactive ion from the bulk to the electrode surface. To numerically solve these equations, we have successfully applied CFD techniques to the electrodeposition model with the general form of convection-diffusion equations.

The transport equation for the conserved quantity per unit mass (ϕ = ionic

concentration(C)/density(ρ) with an external volumetric source term (S_ϕ , with units of conserved quantity per unit volume per unit time) is given by:

$$\rho \frac{\partial \phi}{\partial t} + \rho \nabla \cdot (u\phi) = \rho \nabla \cdot (D_\phi \nabla \phi) + S_\phi \quad (1)$$

where, u is the velocity and D_ϕ is the kinematic diffusivity. The concentration (C) was used as an additional scalar variable of volumetric type.

The choice of spatial coordinate and the boundary conditions depend on the cell geometry and electrode configurations. The transport of the ionic reactant can be tracked by solving an additional set of transport equations, which are fully coupled with the CFD equations during the simulations.

This scalar transport equation was solved for the concentration of the ionic species, with the source/sink (S_ϕ) at the appropriate anode and cathode boundary based on Faraday's law of electrolysis. The electric boundary conditions include the specification of a current flux equivalent to an applied current (i_{app}) through the electrodes with a fixed area. The boundary conditions for the ionic species for the source/sink at the wall of electrodes were calculated as follows:

$$S_\phi = \pm \frac{i_{app}}{zF} \quad (2)$$

where z is the ionic valence and F is the faraday constant. On the anode side, a positive flux is applied, while a negative flux of a same size is applied on the cathode.

The only cathodic electrode reaction to take into account is the deposition of copper ($\text{Cu}^{2+} + 2e^- \rightarrow \text{Cu}$). Since only one single electrode reaction is considered, the deposition efficiency in this model is considered to be 100 % based on the definition of Faraday's law. Assuming that only the reduction of Cu^{2+} takes place at the cathode, Faraday's law gives the total amount of current (I) spent to reduce the equivalent of Cu^{2+} over the effective electrode surface area (A):

$$I = \int idA = i_{ave} \cdot A \quad (3)$$

Here, i and i_{ave} are the local and average current flux for Cu deposition.

No overpotential relation is considered (primary distribution, infinitely fast reaction) at the anode, because the electrochemical processes occurring there are of no interest for this study. Simulations using a fixed anode potential showed that (for the same current) the cathodic current distribution was negligibly affected. This approach allowed the average current density to be fixed in the galvanostatic electrolysis.

The electrode reaction rate is coupled as a gradient of the concentration while the potential gradients, including migration, are neglected. The modeling approach in this study is used to demonstrate the electrode reaction phenomena coupled with the mass transfer in the deposited wall region between the solid boundary and turbulent electrolyte flow.

2.2. Electrode reaction and electric field model

The polarization equation is necessary to express the dependence of the local rate of the electrochemical reaction on the various concentrations and on the potential drop at the interface between the electrode and electrolyte. It is common to use the Tafel approximation [15, 16] of electrode kinetics of the form for metal/ion systems. The local current density (i) distribution on the electrode surface is modelled by the following equation:

$$i = i_0 \left(\frac{C^s}{C^{bulk}} \right) \exp\left(-\frac{\eta}{\beta_C}\right) \quad (4)$$

where, η is the overpotential at the electrode, β_C is the Tafel slope, i_0 is the exchange current density, and superscripts s and $bulk$ are the locations at the electrode surface and bulk electrolyte, respectively.

For electrolyte salt in the interior of an electrolytic cell, there are no free electrical charges. The potential drop across the bulk electrolyte is governed by the Laplace equation [15, 16]:

$$\nabla^2 \phi = 0 \quad (5)$$

where, ϕ represents the local electrical potential. In addition, the current density distribution is obtained by solving the following equation (κ = electrical conductivity):

$$i = -\kappa \nabla \phi \quad (6)$$

Assuming that we impose a specific voltage drop (E_{Cell}) across the electrodes, the overall voltage balance may be written as:

$$E_{Cell} = \phi_{ohm} + \eta_a + \eta_c \quad (7)$$

where ϕ_{ohm} is the ohmic voltage drop, η_a and η_c are the voltage drops owing to activation polarization (i.e., kinetic effects) and concentration polarization (owing to concentration gradients between the electrode surface and bulk electrolyte), respectively.

2.3. Electrowinning cell geometry and boundary conditions for simulation

Copper electrowinning is the process of winning copper from an electrolyte to solid form on a cathode by passing an electric current through the electrolyte to attract copper ions to the cathode. In this demonstration approach, a simple channel cell was selected. Its geometry is rectangular and the distance between the electrodes is a bit large compared to their width. Copper electrowinning takes place in a rectangular channel geometry, with two protruded planar electrodes opposing each other, and the current moves between the electrodes and depletes the copper ions at the cathode.

It may then be assumed that the flow is in a steady state and is turbulent, and incompressible and is between two planar and parallel electrodes. The geometry and generated mesh for this cell is shown in Figure 1.

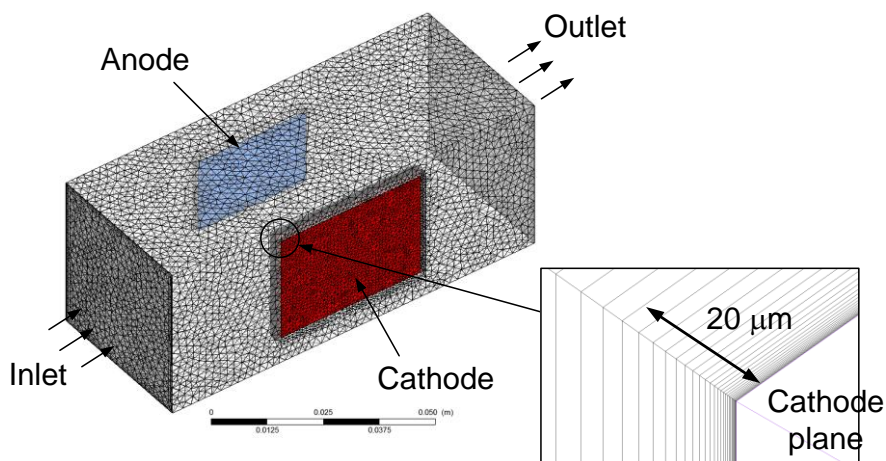


Figure 1. Schematic view of volume-discretized electrowinning cell geometry.

The electrolyte volume was meshed with the tetrahedral elements within the Ansys Workbench platform. In the simulation, the fluid domains of the electrolyte were divided into a diffusion-dominant region near the cathode and a stationary region for the outside, which were connected together with a domain interface. In particular, the fine meshes ($\sim 1 \mu\text{m}$) were applied to the cathode surface to obtain the velocity distribution behaviors and concentration gradient.

Zero gradient boundary conditions for the ion concentration were imposed along the walls except the inlet, outlet and cathode surface. No-slip velocity boundary conditions were applied on all walls. Calculations were initialized with the ion concentration equal to the bulk concentration throughout.

3. RESULTS AND DISCUSSION

3.1 Model parameters and hydrodynamically coupled electro-transport

The relation between electro-transport and mass transport with electrolyte flow during electrolysis was modeled using computational fluid dynamics. In this modeling approach, the electrolyte flow may be considered to be steady, and the fluid is supposed to have a constant chemical composition and physical properties. It was assumed that the aqueous acid electrolyte containing approximately 50 mol/m^3 of cupric ion (Cu^{2+}) was fed into the channel cell at various inlet velocities. Table 1 is the properties of the acid sulfate electrolyte and electrode reaction kinetics used in this simulation [12].

Table 1. Properties and parameters used in the simulation [12]

Electrolyte properties	values
Inlet electrolyte velocity, u (m/s)	0.1-0.5
Initial and inlet concentration of cupric ions, C^{bulk} (mol/m ³)	50
Diffusion coefficient of cupric ions, D_C (m ² /s)	4.2×10^{-10}
Electrolyte density (kg/m ³)	998
Electrolytic conductivity (S/m)	35
Kinematic viscosity, ν (m ² /s)	1.09×10^{-6}
Kinetic parameters for copper deposition	
Tafel slope, b_C (V)	0.0525
Exchange current density, i_0 (A/m ²)	-0.537

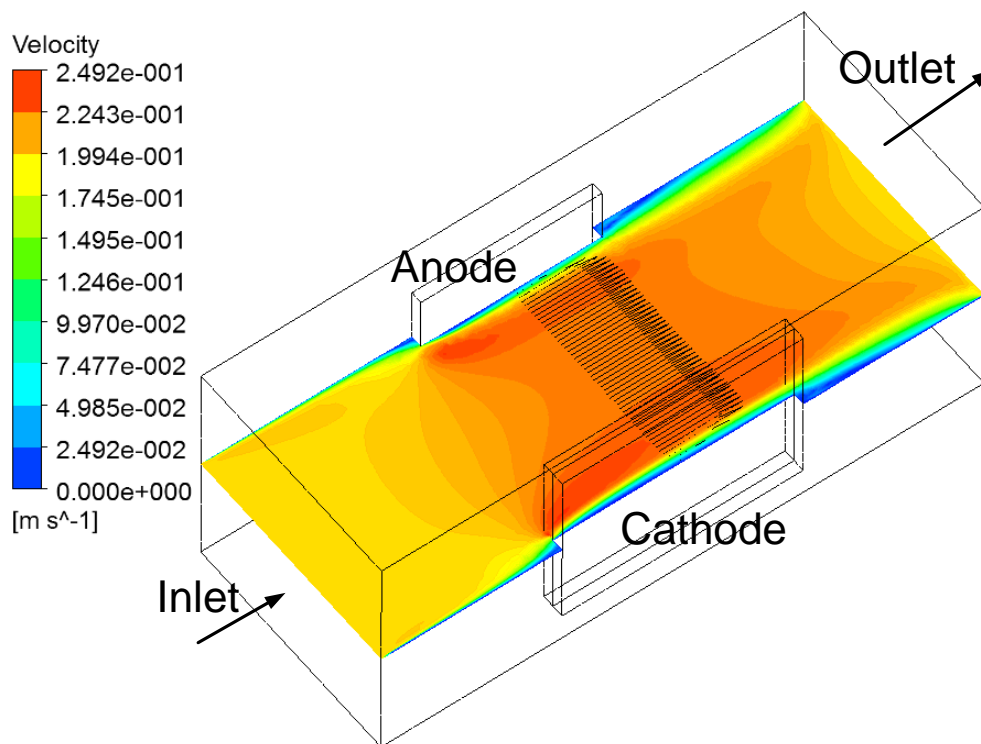


Figure 2. Velocity distribution between the anode and cathode (inlet velocity =0.2 m/s).

The electrolyte solution generally flows between two planar and parallel electrodes. Considering the order of magnitude of the electrolyte velocities, the flows are generally turbulent. It is considered that the cathode is a sink of ion transport as the deposit parallel to the anode. Under these conditions, the modeling for the electrochemical and mass transport phenomena occurring in the cell can be coupled in the CFD platform.

In the model, forced convection by inlet electrolyte is considered. The velocity contours that are flowing at an inlet velocity of 0.2 m/s are shown in Figure 2. From this, the localized velocity values are predicted between the electrodes. The electrolyte velocity profile in a rectangular channel cell under a pressure-driven hydrodynamic flow shows parabolic patterns with a wide plateau. The maximum velocity was found at the region between the electrode and center of the channel, because of

the electrodes projecting out over the channel. The velocity was almost zero at all of the channel walls. However, the fully developed parabolic profile patterns were not found at the inlet or outlet region within the channel.

In this study, we modeled the stationary flow-assisted mass transport that controls the electrode reaction rates in an electrochemical system using a CFD based electrochemical simulation approach. Hence, it is necessary to know the concentration distribution of electrolyte ions in the vicinity of the electrode surface at various flow velocities, which precludes using the coupled transport equation for convective diffusion. To develop a comprehensive modeling approach, we focused our attention on the deposition of copper at the cathode in this simulation. A concentration sink flux equivalent to the current density was applied at the cathode.

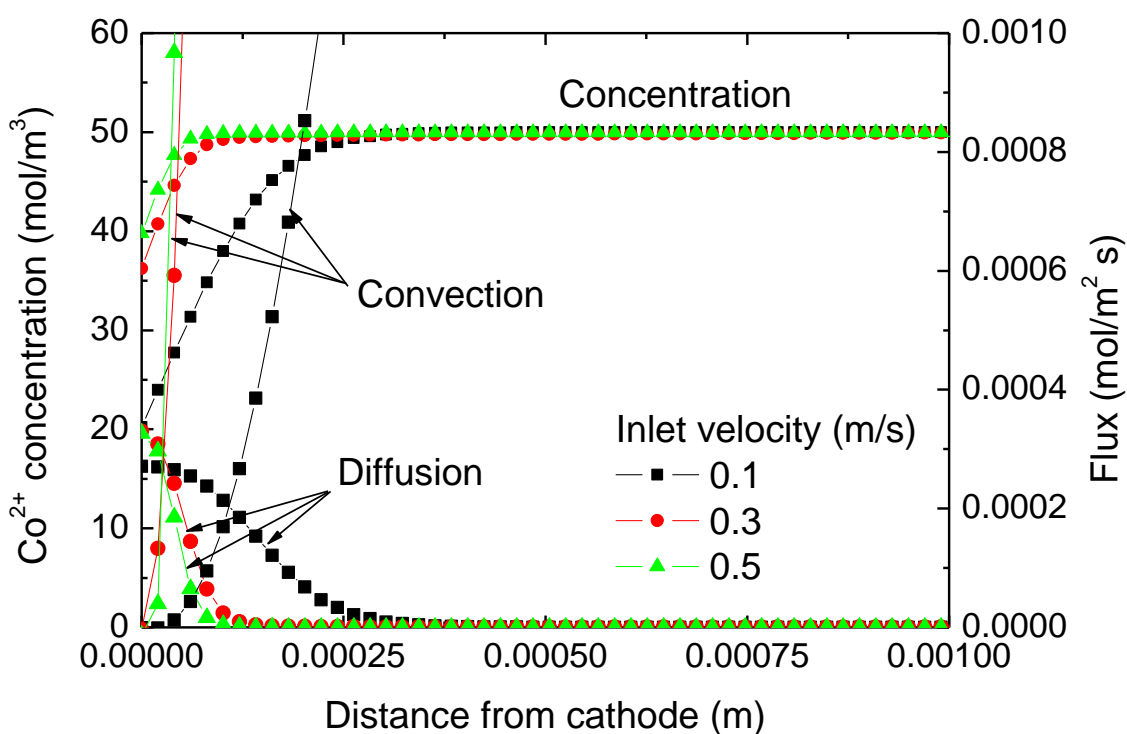


Figure 3. Concentration and mass transport (convection and diffusion) profiles close to the cathode with three electrolyte flow conditions (0.1, 0.2 and 0.3 m/s).

During electrolysis, cations (Cu²⁺) have to be transported from bulk electrolyte to the cathode surface. In general, this mass transport occurs by diffusion, convection, and migration. Close to the electrode surface, the primary mass transport process is diffusion. At an electrolyte region near the cathode, the diffusion flux is the dominating transport mechanism, while the convection is the dominant flux in the bulk electrolyte, as shown in Figure 3. The copper ion concentration decreases with a decreasing distance from the cathode owing to its ion consumption with the electrode reaction. An increasing flow velocity results in an increase in surface concentration.

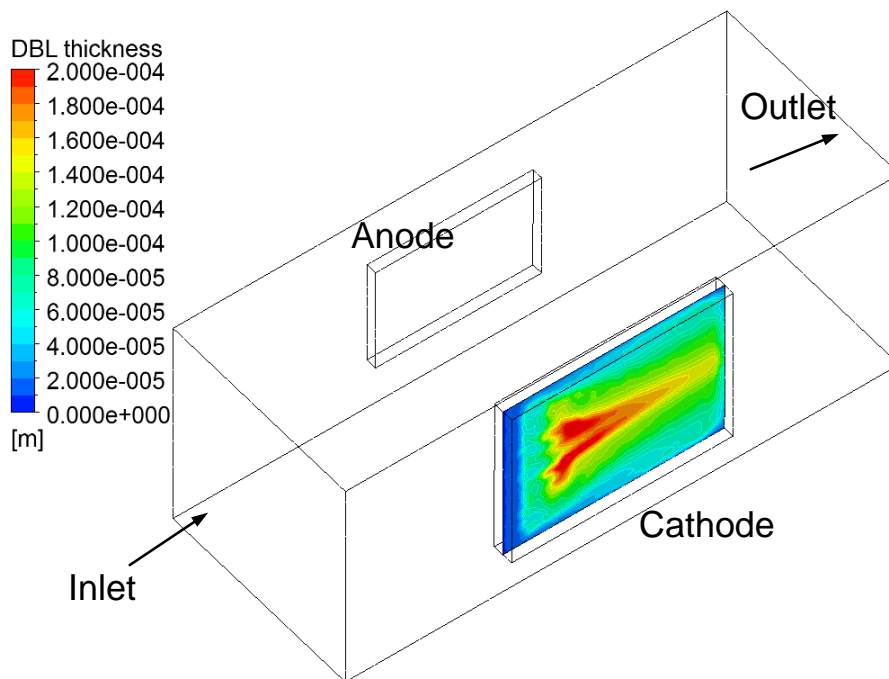


Figure 4. Diffusion boundary layer thickness at the cathode ($i_{app}=100 \text{ A/m}^2$, inlet velocity =0.2 m/s).

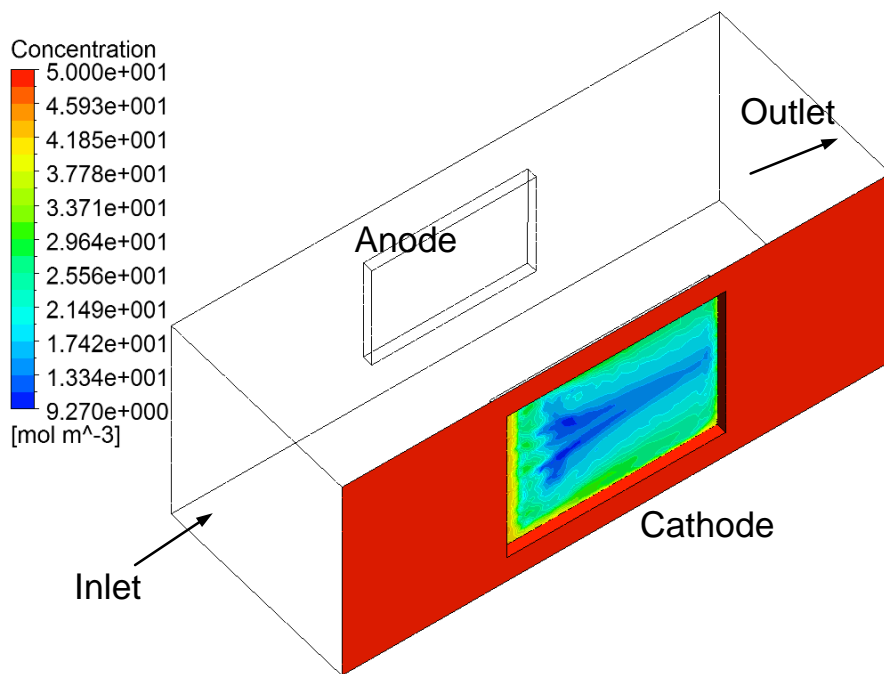


Figure 5. Surface concentration distribution at the cathode and side channel wall ($i_{app}=100 \text{ A/m}^2$, inlet velocity =0.2 m/s).

The distribution of the diffusion boundary layer thickness was simulated at the cathode surface, as depicted in Figure 4. A higher thickness value of the diffusion boundary layer gives rise to a decreased surface concentration as shown in Figure 5.

3.2 Mass transport-coupled electric field analysis

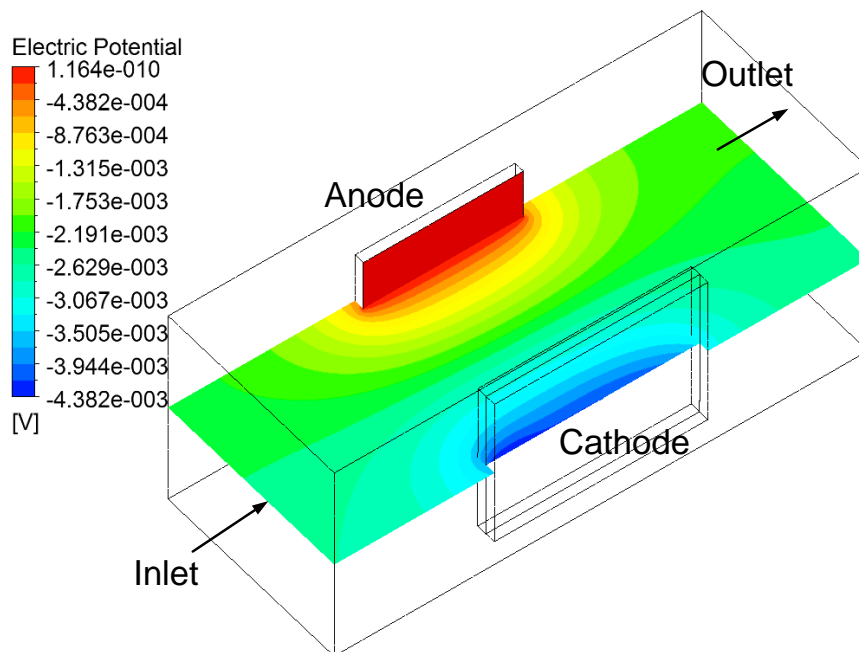


Figure 6. Electric potential distribution between the anode and cathode ($i_{app}=100 \text{ A/m}^2$, inlet velocity =0.2 m/s).

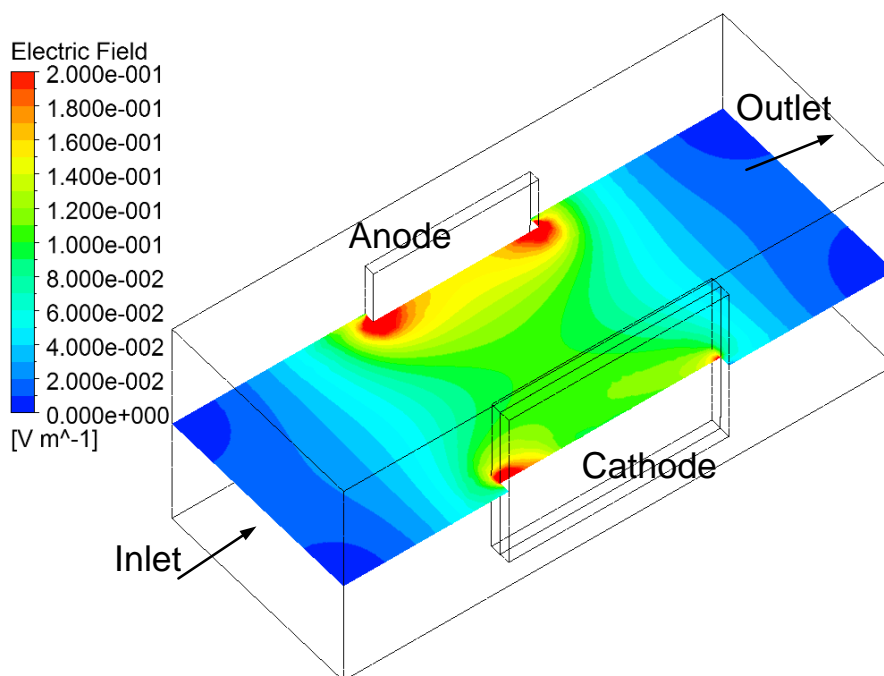


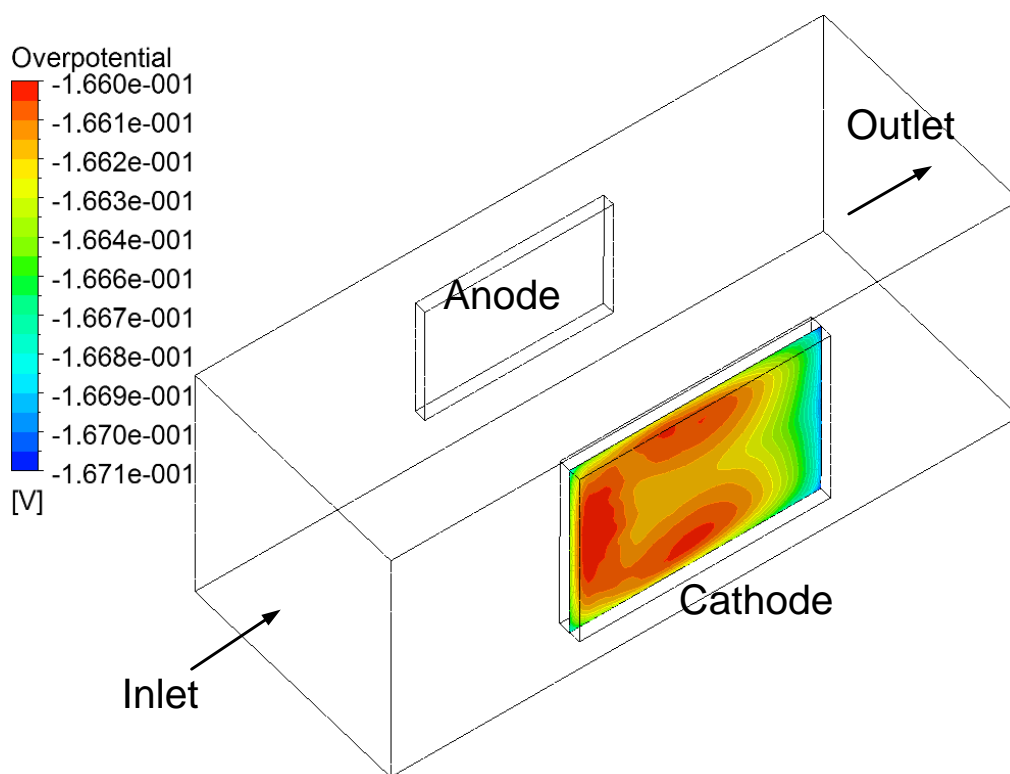
Figure 7. Electric field distribution between the anode and cathode ($i_{app}=100 \text{ A/m}^2$, inlet velocity =0.2 m/s).

Metal ion reduction at the cathode yields a decrease in the ion concentration, which reduces the electrode reaction rate. Although the current distribution at the anode as a counter electrode will be

non-uniform under a real situation, this is found to have a negligible effect on the rate of the cathode. Accordingly, the simulation approach using a fixed anode potential shows that (for the same current) the cathodic current distribution is negligibly affected [12]. This approach allows the average current density to be fixed. Based on the conservation of charge, the numerically simulated average current on the cathode should be equal to the total current on the anode.

If the deposition rates at the cathode side are focused on the modeling approach, the rate of the anodic reaction can be assumed reversible under a constant applied current condition. This assumption is the ideal case of no surface overpotential at the anode. Figure 6 shows the electric potential distribution patterns (cross section view) coupled with the cathode overpotential through the electrolyte region between the anode and cathode. Since herein it is assumed that the anode is grounded as 0 V, the potential at the cathode can be calculated from the given flux-out (current density from Tafel kinetics) using mixed boundary conditions. Owing to the electric conductivity of the electrolyte, there is a potential increase toward the grounded anode. This is the ohmic potential drop, which is the loss associated with resistance to the electron transport in the electrolyte region. A simulation of the electric field between the electrodes is also shown in Figure 7. Spatial current densities are locally proportional to these gradients of potential. These results show the case of a coupled computation with the concentration gradient and surface overpotential.

3.3 Local current density and overpotential



(a)

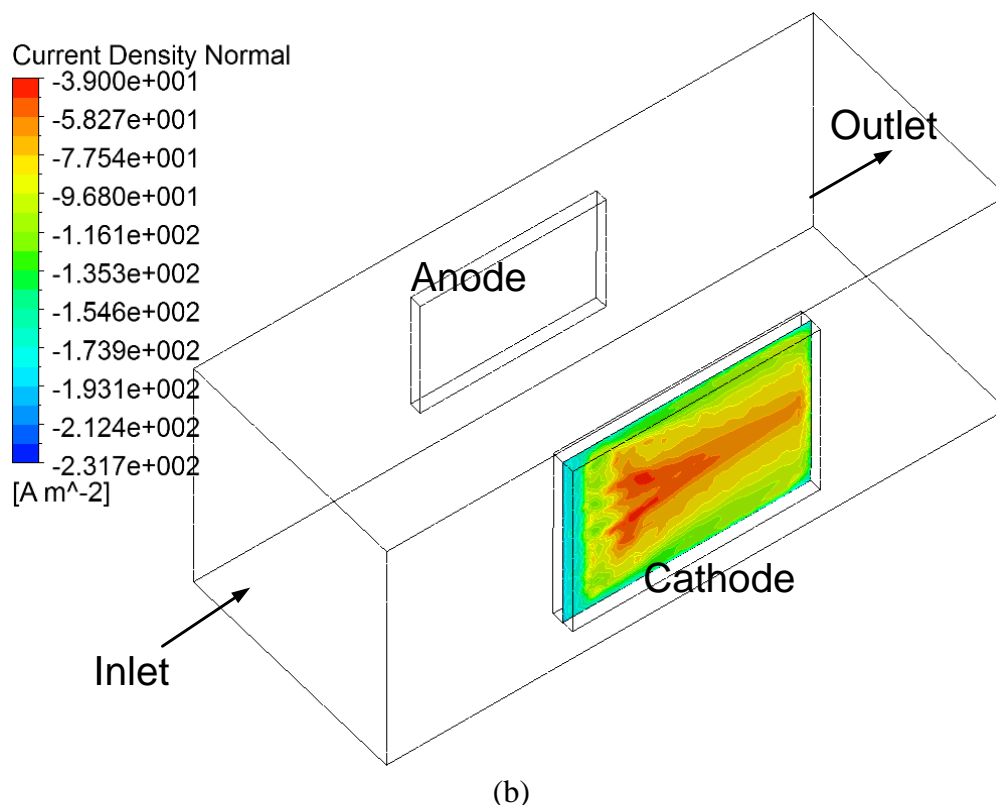


Figure 8. Local overpotential (a) and current density (b) at the cathode surface ($i_{app}=100 \text{ A/m}^2$, inlet velocity =0.2 m/s).

In addition, the model can provide many more details on the mass transport controlled electrochemical characteristics occurring in an electrowinning cell. An increased diffusion boundary layer leads to a higher overpotential in this electrode region. Accordingly, an increased inlet velocity condition results the decreased overpotential owing to a smaller diffusion boundary layer thickness. In Figure 8, the distribution of overpotential (a) and local current density (b) throughout the cathode surface are provided for the case of a current density of 100 A/m^2 and an inlet velocity condition of 0.2 m/s . The effects of electrolyte concentration are taken into account in this simulation. It was found that a higher local overpotential arises from a lower ionic concentration at the electrode surface. Under this condition, there is not a large potential drop in the electrolyte bulk. Thus the diffusion transport has a dominant control factor at the electrode surface. It is shown that the increased inlet velocity condition gives a decreased surface overpotential and has less of an effect on the ohmic drop. This is evident from the modified Tafel kinetics, which is a function of the overpotential and surface concentration, as in Equation (4). Accordingly, to maintain the given current density, a higher overpotential is necessary for the compensation of the ionic reactant depletion.

The diffusion boundary layer (δ) is defined in the literature [17]. Once we know the local diffusion boundary layer, the current density can be locally estimated according to Fick's law, as in Equation (8):

$$i = -zFD_C \left(\frac{\partial C}{\partial x} \right)_{x=0} \approx -zFD_C \frac{C^{bulk} - C^s}{\delta} \tag{8}$$

Since Equation (8) serves to define the diffusion boundary layer thickness, it can be obtained from the local concentration gradients in the direction normal to the electrode surface. Close to the cathode surface, the primary mass transport for an electro-transport process is diffusion control. Local current density can be approximated according to Fick’s law as expressed in Equation (8). Once a concentration gradient in the direction normal to the cathode is obtained from the mass transport simulation, the diffusion boundary layer thickness (δ) is able to be estimated from the definition as the intersection between the tangent at the concentration distribution and concentration of the bulk electrolyte.

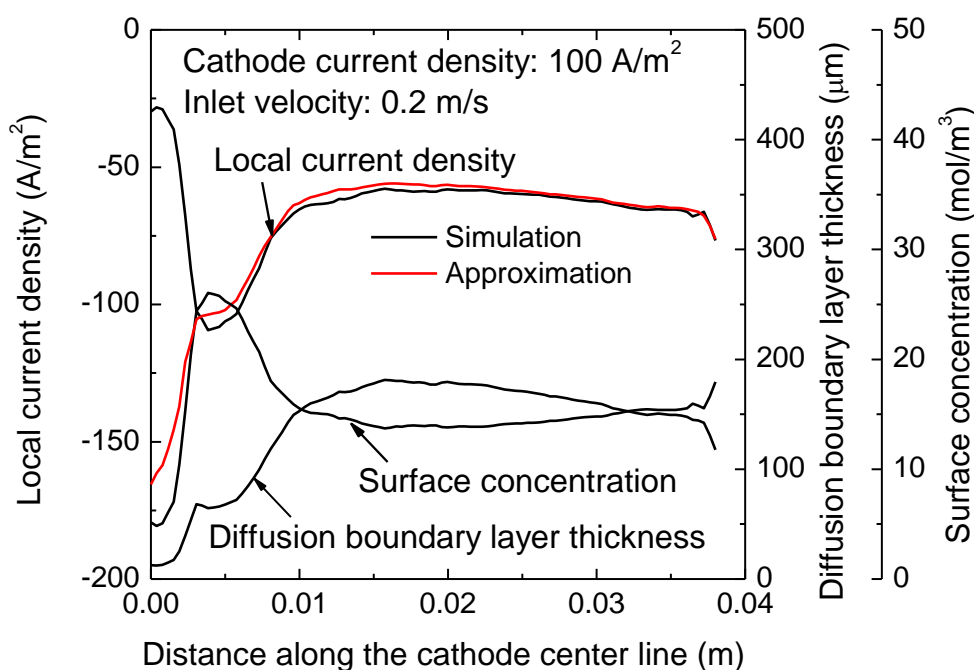


Figure 9. Simulation and approximated local current density along the center line of cathode ($i_{app}=100$ A/m², inlet velocity =0.2 m/s).

Figure 9 shows a comparison of the local current density between the simulation and approximation from the diffusion boundary layer thickness for an applied current density of 100 A/m² and inlet velocity condition of 0.2 m/s. In this figure, the local current densities were drawn on the center line along the cathode surface. The approximated local current density indicates a fairly good agreement with the simulation results along most of the cathode surface. However, as an approximation was considered on the concentration gradient along the normal direction to the cathode, a slight difference was found in the vortex region of the electrolyte facing the protruded cathode.

Figure 10 shows a variation of current density as a function of overpotential based on the

average values of the diffusion boundary layer thickness throughout the cathode. The curves were obtained by the relationship between the current density and overpotential with the values of the diffusion boundary layer thickness estimated from the concentration profile for various inlet velocities. The simulated polarization curves clearly show the charge transfer, mixed (charge transfer and mass transport) and mass transport controlled region.

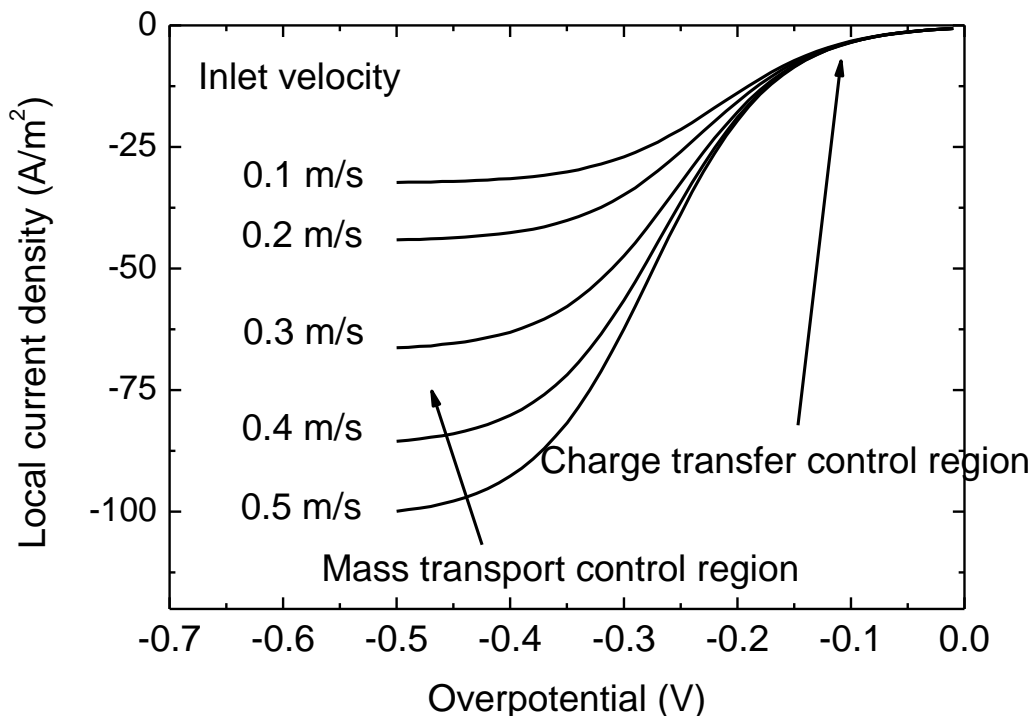


Figure 10. Local current density as a function of overpotential at various inlet velocities (0.1-0.5 m/s).

In the charge transfer controlled region, the electrolyte turbulence has little effect on the voltage drop. In this simulation condition, the polarizations with a lower exchange current density would play a significant role in the total losses causing a potential drop from the ideal voltage. It was simulated that the overpotential contributed to most of the cell potential under this demonstration condition.

The above simulations provide a good illustration of the capabilities of the present modeling approach. The proposed CFD model was shown to be able to predict not only the convective diffusion behavior of the ionic reactants but also the mass-transport limited electrochemical polarizations. It was found that the flow characteristics of the electrolyte influenced the diffusion-limited current density and electro-winning deposit. To evaluate these influences, a coupled approach of the multiphysics simulation for the flow and ion transport is necessary. In addition, more detailed analyses and benchmarking tests are desirable to fully investigate a validation study.

4. CONCLUSIONS

This study demonstrated a modeling approach based on the full coupling of electrochemical reactions with a mass transport of ionic species using a commercially available CFD platform. An analysis was carried out for the case of copper electrowinning from a flowing cupric acid electrolyte through the simplified channel cell with planar and parallel electrodes. The demonstrations presented here have focused only on copper deposition during steady-state electrolysis. A finite volume numerical scheme based the CFD technique was successfully adapted to simulate 3-dimensional behaviors of the electrochemical cell. The CFD model was shown to be able to predict not only the convective diffusion behavior of the ionic reactants but also the mass-transport limited electrochemical polarizations. This comprehensive model provides valuable information on the transport phenomena inside an electrolytic cell such as the ion concentration, electric potential and local current density distribution under a given current driven condition. Future work will focus on the benchmarking of this model to validate with a proven electroplating system that controls the fluid dynamics and mass transport conditions.

ACKNOWLEDGMENTS

This work was supported by the National Research Foundation of Korea (NRF) grant funded by the Korea government (MSIP).

References

1. T. Storck and A. A. Wragg, *J. Appl. Electrochem.*, 21 (1991) 463.
2. P. Mandin and J. Deconinck, *Electrochemical engineering modeling and numerical simulation to improve the presentation of electrochemical cells and diagnostic techniques*, Abstract #2661, *Proceedings 214th ESC Meeting*, Honolulu, Hawaii, October 12-17 (2008).
3. P. Mandin, J. M. Cense, G. Picard and D. Lincot, *Electrochim. Acta*, 52 (2006) 1296.
4. P. Mandin, J. M. Cense, C. Fabian, C. Gbado and D. Lincot, *Comput. Chem. Eng.*, 31 (2007) 980.
5. P. Mandin, R. Wüthrich and H. Roustan, *Comput. Aided Chem. Eng.*, 17 (2009) 435.
6. M. F. Santillo, A.G. Ewing and M. L. Heien, *Anal. Bioanal. Chem.*, 399 (2011) 183.
7. S. V. Patankar, *Numerical Heat Transfer and Fluid Flow*, McGraw-Hill Book Company, New York, (1980).
8. P. Mandin, J. M. Cense, B. Georges, V. Favre, T. Pauporte, Y. Fukunaka and D. Lincot, *Electrochim. Acta*, 53 (2007) 233.
9. C. W. Wang, F. Albano and M. Sastry, *Computational method for design and manufacture of electrochemical systems*, *United States Patent*, US 7,945,344 B2 (2011).
10. B. E. Conway and R. E. White, *Modern Aspects of Electrochemistry*, Kluwer Academic/Plenum Publisher, New York (2002).
11. E. Malyshev, U. Landau and S. Chivlikhin, *Modeling the deposit thickness distribution in copper electroplating of semiconductor wafer interconnects*, Paper 190 b, Session TK, *Proceedings of the AIChE Annual Meeting*, San-Francisco, CA, November 16-21 (2003).
12. C. T. J. Low, E. P. L. Roberts and F. C. Walsh, *Electrochim. Acta*, 52 (2007) 3831.
13. C. T. J. Low and F. C. Walsh, *Surf. Coat. Tech.*, 202 (2008) 1339.
14. ANSYS CFX Release 12 User's Guide, ANSYS, Inc. (2009).
15. A. J. Bard and L. R. Faulkner, *Electrochemical Methods, Fundamentals and Applications*, 2nd

edition, John Wiley & Son Inc., New York (2001).

16. D. J. Pickett, *Electrochemical Reactor Design*, American Elsevier Inc., New York (1979).

17. K. Filzwieser, K. Hein and G. Mori, *JOM*, 54 (2002) 28.

© 2013 by ESG (www.electrochemsci.org)